

Time-Dependent FEM Simulation of Dilution Control of Laser Cladding by Adaptive Mesh Method

Jae-Do Kim,* Yun Peng

(Department of Mechanical Engineering, Inha University)

Dilution is an important factor which influences the properties of clad layer. In this paper the change of dilution during laser cladding and the control of dilution are simulated by a finite element method. The adaptive mesh method is adopted for the time-dependent finite element method computation so that the shape of melt pool can be well represented. The situation of the width control of melt pool is also simulated, which indicates that the dilution can be controlled if the width of melt pool is controlled. Computational results indicate that if a line energy (input energy per unit distance) remains constant the dilution will increase with time, especially at the beginning. Simulation results show that it is possible to control dilution in a certain range if the line energy decreases with time. Experiment of Nd: YAG laser cladding with wire feeding is performed. Experiment results coincide well with the FEM results.

Key Words : FEM, Adaptive Mesh, Laser Cladding, Dilution

Nomenclature

k : Thermal conductivity
 ρ : Mass density
 c : Specific heat
 h : Convective heat transfer coefficient
 T : Temperature
 T_m : Melting point
 T_0 : Ambient temperature
 P : Laser power
 v : Cladding speed
 f : Absorbed power density
 \underline{M} : Heat capacity matrix
 \underline{K} : Conductivity matrix
 \underline{F} : Nodal force vector

1. Introduction

Laser cladding is used in two respects: production of parts of the composite materials and the repair of the worn parts. In the former case the

performance can be improved and/or cost can be reduced by the savings of expensive metals. In the second case the repair cost may be significantly less than replacement cost or time can be saved. Laser beam is a power of high energy density, which allows the rapid transfer of heat to the materials being processed with minimum conduction into the adjacent base metal, resulting in low total heat input. Low distortion and reduced cracking susceptibility can be realized by laser cladding. Rapid solidification of the melt pool also provides the potential of developing coatings with the non-equilibrium microstructures and the superior physical properties. In the automobile industry the laser cladding has been used for cladding on the selected areas of valves, shafts, and other engine components to improve wear and high temperature corrosion resistance. The power utility industry has begun to use the laser cladding of boiler tubes in the steam generators. Laser cladding has also been used for the repair of jet and power turbine engine shaft and blade components. (Koshy, 1985; Kim and Subramanian, 1988; Ramous et al., 1989; Mazumder et al., 1992; Kim et al., 1992; Denney and Duhamel, 1998; Kim et al., 1998)

* Corresponding Author,

E-mail : kimjaedo@inha.ac.kr

TEL : +82-32-860-7316 ; FAX : +82-32-868-1716

Department of Mechanical Engineering, Inha University, 253 Yonghyun-dong, Nam-Ku, Incheon 402-751, Korea. (Manuscript Received April 27, 1999; Revised November 24, 1999)

To get high quality clad layer, low dilution is required. If the melt pool is severely diluted the properties of clad layer will be influenced. Some researchers engaged in experimental research in dilution (Atamert and Bhadeshia, 1989; Hirose et al., 1992; Uenishi and Kobayashi, 1993; Liu, Damborene et al., 1993; Mazumder and Shibata, 1994; Fouquet et al., 1994; Tosto et al., 1994; Yellup, 1995) and solidification behavior of melt pool (Mohanty and Mazumder, 1998). In the field of mathematical modeling, composition of metastable alloy of extended solid solution (Mazumder and Kar, 1987; Kar and Mazumder, 1988; Kar and Mazumder, 1989), convection in melt pool (Chan et al., 1984; Yang et al., 1992), quasi-steady temperature field (Hoadley and Rappaz, 1992), solidification conditions (Frenk et al., 1993) and non-equilibrium phase diagram (Agrawal et al., 1993) were modeled.

During laser cladding, heat will accumulate near the melt pool before quasi-steady state is reached. So the dilution will become larger and larger. To keep low dilution, the input energy density (input energy per unit area) should be reduced. In this paper, the change of dilution during laser cladding is computed and the control of dilution is simulated by the time-dependent finite element method with the adaptive mesh.

2. Physical Model

Figure 1 shows the physical model. Laser beam with uniformly distributed power strikes on a rectangular area of base metal and moves relative to it. Cladding material is filled into the melt pool. The height of clad layer depends on the feed speed of cladding material. If we adapt the feeding speed to the width of clad layer, the height of clad layer can be kept constant. Here we adopt a constant height of clad layer. The width of clad layer changes during cladding according to the change of thermal field of the base metal. The shape of the clad layer depends on the physical properties of cladding material and base metal. Here we assume that the upper surface of clad layer is a plane and the parts between the upper surface of clad layer and the base metal surface

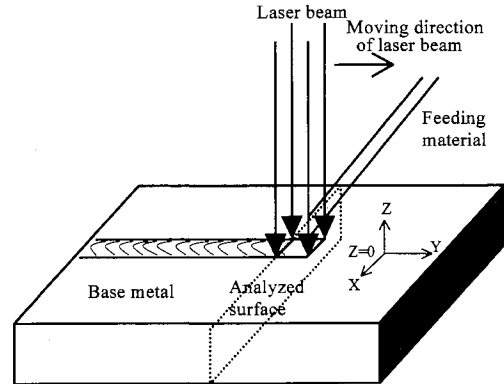


Fig. 1 Schematic diagram of the model

are composed of a series of curves which are in the shape of a quarter circle. The point where the clad layer connects with the base metal is assumed to be at the surface point of base metal where the melting line locates in.

The basic assumptions for the model are:

(1) The thermal conductivity, specific heat and density are independent of temperature. Actually, these parameters are affected by temperature in different degrees. Because of the difficulty of getting all the exact data in every temperature point, the parameters are adopted to be the values at the average temperature.

(2) In melt pool these parameters are proportional to the volume fractions of cladding material and base metal. Because the melt pool is composed of the mixture of base metal and cladding material and there is no chemical reaction between them, this is an assumption with sound reason.

(3) Latent heat effects are neglected because for the relatively small volume of melt pool latent heat of fusion is compensated by latent heat of solidification.

(4) The effect of convection of liquid metal in the melt pool is neglected. Because (a) the heat source is highly concentrated and moving, and (b) the melt pool is small enough compared to the volume of base metal, the speed of liquid convection is much slower than the speed of heat conduction and its effect is small.

(5) Near the end part of the melt pool heat conduction is in the transverse sections perpendicular to the moving direction.

ular to the cladding direction and before or behind this section heat conduction is three-dimensional. For a moving heat source projecting on a base metal, the overall heat flow is three-dimensional. But near the end of melt pool heat flow is essentially in the transverse cross section because the temperature gradient in the transverse cross section is much larger than that in the longitudinal section (David and Vitek, 1989).

The reference frame is set to attach to the laser beam.

3. Formulation and the Adaptive Mesh

The energy equation is

$$\underline{M}\dot{\underline{T}} + \underline{K}\underline{T} = \underline{F}$$

Let t_n denote a typical time in the response so that $t_{n+1} = t_n + \Delta t$, where $n=0, 1, 2, \dots, N$. Introduce a parameter θ such that $t_\theta = t_n + \theta \cdot \Delta t$, where $0 \leq \theta \leq 1$. We can write the above energy equation at t_θ as:

$$\underline{M}\dot{\underline{T}}_\theta + \underline{K}\underline{T}_\theta = \underline{F}(t_\theta)$$

Introduce the approximations:

$$\dot{\underline{T}}_\theta = \frac{\underline{T}_{n+1} - \underline{T}_n}{\Delta t}$$

$$\underline{T}_\theta = (1 - \theta) \cdot \underline{T}_n + \theta \cdot \underline{T}_{n+1}$$

$$\underline{F}(t_\theta) = (1 - \theta) \cdot \underline{F}(t_n) + \theta \cdot \underline{F}(t_{n+1})$$

we have:

$$\underline{K} \cdot \underline{T}_{n+1} = \underline{F}_{n+1}$$

where

$$\underline{K} = \theta \cdot \underline{K} + \frac{1}{\Delta t} \underline{M}$$

$$\underline{F}_{n+1} = \left[-(1 - \theta) \cdot \underline{K} + \frac{1}{\Delta t} \underline{M} \right] \cdot \underline{T}_n + (1 - \theta) \cdot \underline{F}_n + \theta \cdot \underline{F}_{n+1}$$

The absorbed power density f is calculated by the following formulation:

$$f = \eta \times P / [W \times (L + v)]$$

where L is the spot length (in the cladding direction), W is the spot width (transverse to the cladding direction), and η is the absorptivity of laser power, which is dependent on the materials and their surface condition of base metal and feed

materials, such as surface finishing, oxygen content, and the flow rate of assisting gas (Liu et al., 1994; Ono et al., 1987).

The dilution is calculated by the following formulation:

$$\text{Dilution} = \frac{\text{(area of melted base metal)}}{\text{(area of melt pool)}}$$

Because the shape of melt pool and the width of clad layer changes during cladding, it is necessary to adapt the mesh to the instant shapes of melt pool and the width of clad layer, so that the mesh can represent the changing shape of the modeled object during cladding. To implement above, we preset an assumed melting line and clad layer width. After one round computation we get a computed melting line and clad layer width. By comparing the preset melting line and clad layer width with the computed values we reset a new melting line and new clad layer width and adapt the mesh accordingly. Then we do the computation again. These steps repeat until the difference between computed melting line and preset melting line is smaller than a limit (here the error limit is adopted to be 0.0001 mm). The method of mesh adaptation can be expressed as:

$$x_{n+1} = x_n + \omega \cdot (x_m - x_n)$$

$$y_{n+1} = y_n + \omega \cdot (y_m - y_n) \quad (0 < \omega < 1)$$

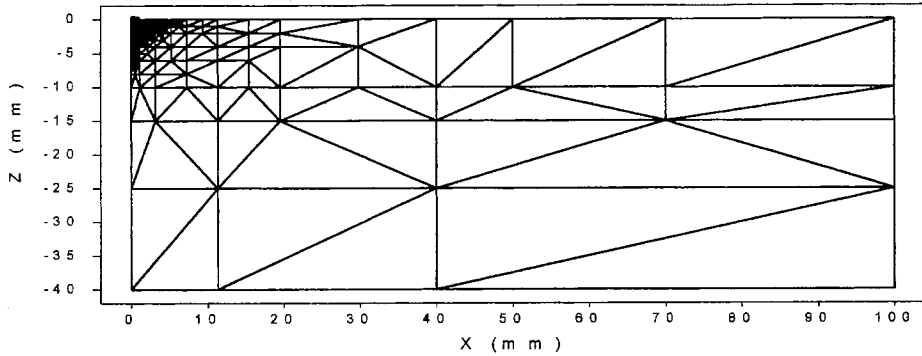
where (x_m, y_m) are computed values.

The FEM computation has been done by C language programming. Table 1 shows the physical properties used for the computation.

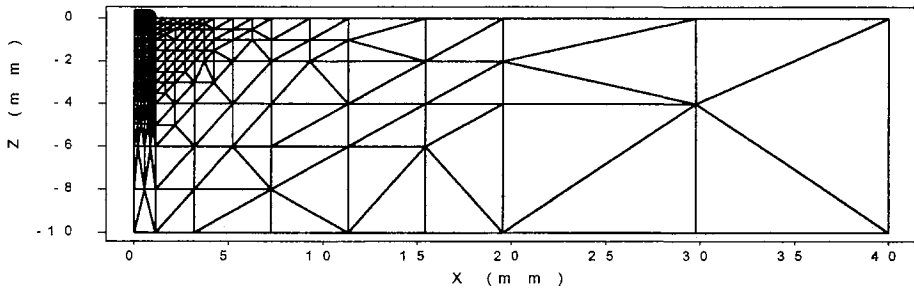
Figure 2 shows the original mesh. Because of the symmetry of thermal field in the section, only half of the section is meshed. A mesh composed of

Table 1 Physical properties of cladding material and base metal

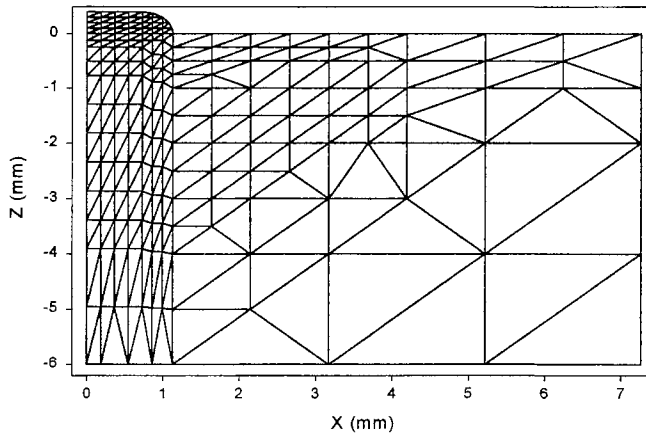
	Inconel 600	Mild steel	Al	Inconel 690
k (W/m·k)	23	74.1	225	37.7
h (W/m ² ·k)	100	100	100	100
T _m (k)	1643	1803	933	1555
ρ (kg/m ³)	8420	7870	2385	7950
c (J/kg·k)	580	482	1067	836



(a) Original mesh



(b) Part magnification



(c) Larger part magnification

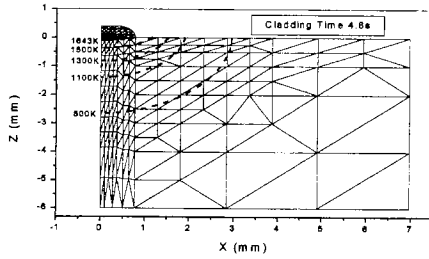
Fig. 2 Original mesh

432 triangle elements is adopted for the computation. During computation the mesh adapts its shape and position according to the shape of melt pool and the width of clad layer automatically. Figure 3 shows the variations of thermal field with cladding time for laser cladding with and without dilution control, and the automatically adapted mesh with the variation of melt pool

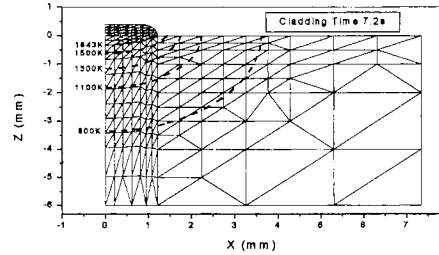
shape.

4. Experiment Equipment and Materials

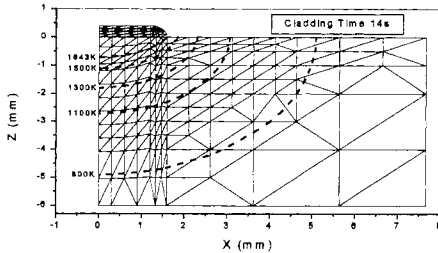
Laser cladding with wire feeding is done by Nd: YAG laser power. The parameters used for the experiment are: beam mode: TEM₀₀, fre-



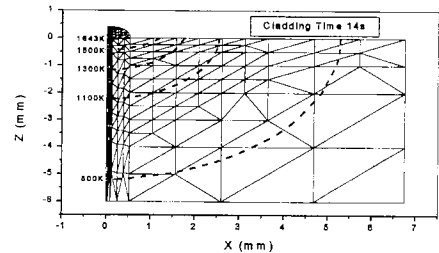
(a) Cladding time 4.8s, without dilution control



(b) Cladding time 7.2s, without dilution control



(c) Cladding time 14s, without dilution control



(d) Cladding time 14s, with dilution control

Fig. 3 Meshes and thermal fields at different cladding time for cladding Inconel 690 on Inconel 600, without and with dilution control

quency: 20Hz, peak power: 5.5 KW, duty cycle: 4%, average power: 220 W. Optical fiber is used to conduct the laser beam. Beam diameter is 2.5 mm. Ar is used as shielding gas to protect the melt metal and cooling of the nozzle of laser beam. Inconel 600 wire of 0.2 mm diameter is used as the feeding wire. Inconel 600 plate is used as the base metal. Wire feeding speed is kept constant while cladding speed is changed.

5. Results and Discussion

5.1 Dilution of laser cladding

5.1.1 FEM results

The laser beam is assumed to strike perpendicularly on the base metal and is distributed uniformly in a rectangle area of 3 mm × 3 mm. The absorptivity of laser power is dependent on the materials and their surface condition of base metal and feed materials, such as surface finishing, oxygen content, and the flow rate of assisting gas (Ono et al., 1987; Liu et al., 1994). Here it is assumed that 60% of the laser power is absorbed by the base metal and cladding material (Li and

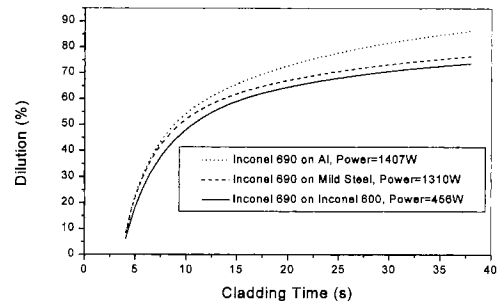


Fig. 4 The variation of dilution of clad layer using constant power

Mazumder, 1984). The size of cross section of the base metal perpendicular to the cladding direction is a rectangle of 200 mm × 40 mm. The cladding material is Inconel 690 and base metals are Inconel 600, mild steel and Al, respectively. The ambient temperature is adopted to be 298 K.

Figure 4 shows the changes of dilution of clad layer during cladding for the constant line energy (energy per unit distance), where the cladding speeds are all at 3.33 mm/s for cladding Inconel 690 on Al, mild steel and Inconel 600. The laser powers needed to melt the base metal in 4 seconds are different for Inconel 600, mild steel and Al.

The laser power needed for Al is higher than that for mild steel, although the melting point of Al (933k) is much lower than that of mild steel (1803k), and the power needed for steel is higher than that for Inconel 600. The cause is that the heat conductivity of Al is much higher than that of mild steel, and the heat conductivity of mild steel is higher than that of Inconel 600. For all of the three cases, the dilutions increase rapidly at first. Then their increase rates become slower and slower. The increase rate of dilution of Al is higher than that of mild steel and Inconel 600. After 38 seconds of cladding time, the dilutions of melt pool are still changing. The results indicate that quasi-steady thermal field can not be reached in a short time. It also implies that to maintain small dilution, the input line energy should be reduced with cladding time.

5.1.2 Experiment results

Figure 5 (a) and (b) shows two cross sections of a clad layer which are 5mm and 25 mm from the beginning of clad layer, respectively. It is seen that the depth and dilution of clad layer at 25mm from the beginning is much larger than that at 5mm from the beginning. Observation of the cross section of clad layer also indicates that the width of clad layer is different from the width of melt pool in the base metal. With the increase of

distance from the beginning of clad layer, the width of melt pool in the base metal increases significantly, but the width of clad layer shows little change.

The changes of width and depth of melt pool are because of the accumulation of heat near melt pool during cladding. These results correspond to that of FEM analysis. The very slow change of width of clad layer results from the constant wire feeding volume per unit distance because the shape of clad layer is not changed significantly. During cladding, part of the melt metal flows beyond the width of melt pool in the base metal and bond with the base metal during cooling.

Figure 5 (b), (c), (d) shows the cross sections of melt pool at different cladding speeds. It is indicated that the width of clad layer is wider than the melted width of base metal. That's because part of melted metal flows beyond the melting line of base metal and bonds with the base metal by the heat of melted metal. Figure 6 shows the variation of width and depth of melt pool resulted from experiment study and finite element analysis. With the increase of cladding speed, the width of melted base metal, the width of clad layer, and the depth of melt pool decrease. The decreases of width of melted base metal and depth of melt pool result from the decrease of input line energy with the increase of cladding speed. The decrease of width of clad layer is because of both the decrease of wire feeding volume per unit distance and the decrease of input line energy with the increase of cladding speed. The FEM results coincide well with the experiment results.

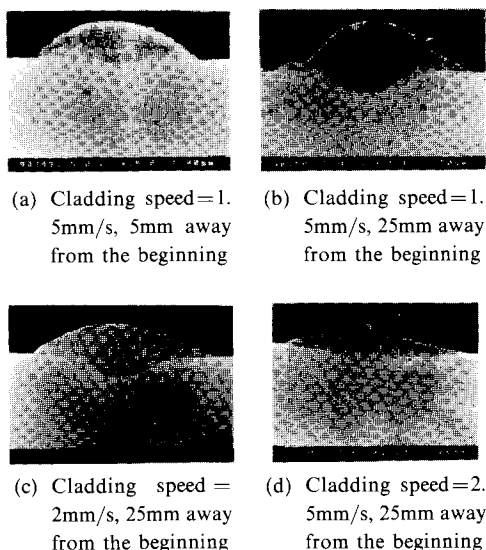


Fig. 5 Cross sections of clad layers

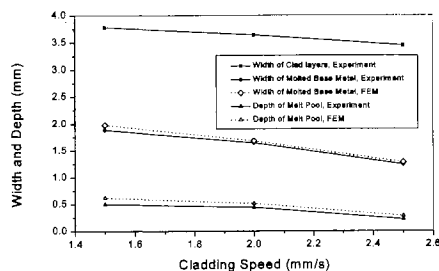


Fig. 6 Width and depth of melt pool at different cladding speed at the cross section 25mm away from the beginning

Above results imply that one way to maintain low dilution during cladding is to adapt (decrease) the input line energy with cladding time so that the depth of melt pool can be kept low and make the molten metal to bond with the base metal by the heat of melted metal.

5.2 Simulation of dilution control

The flowchart of program for dilution control is shown in Fig. 7. At a given cladding time, the dilution of melt pool is computed. Then the input power is adapted by comparing the computed dilution with preset dilution limit. That is:

$P = P - \Delta P$, if the computed dilution is larger than the preset dilution limit.

$P = P + \Delta P$, if the computed dilution is smaller than the preset dilution limit.

where P is the energy density absorbed by the

base metal.

This process repeats until the computed dilution is in the preset dilution limit. Then the computation goes to the next time step and the above process repeats again.

Figure 8 shows the realized dilution of clad layer. Here the controlled dilution is preset between 7.95% and 8.05%. The resulting depth and width of melt pool during cladding are shown in Fig. 9. Under the condition of controlled dilution, both of the depth and width are constant during cladding. The results indicate that if the dilution is controlled, the thermal field is also controlled. It is also seen that under the formerly suggested cladding condition the depth of melt pool is much smaller than the width.

Figure 10 shows the resulting laser powers for controlling the dilution when cladding speeds are all at a constant value of 3.33 mm/s for cladding of Inconel 690 on Al, mild steel and Inconel 600. For all of the three cases, the laser powers decrease rapidly at first. Then their decrease rates become slower and slower. To get the same dilution, the laser power needed for cladding of

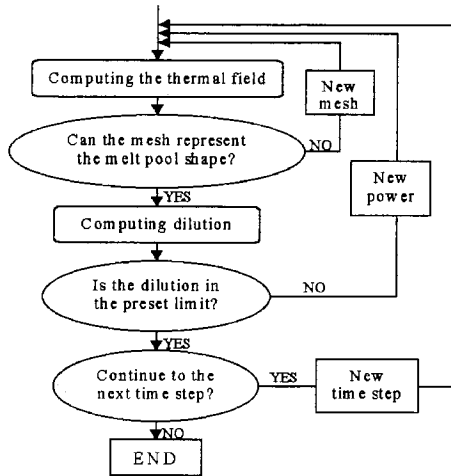


Fig. 7 Flowchart of program for dilution control

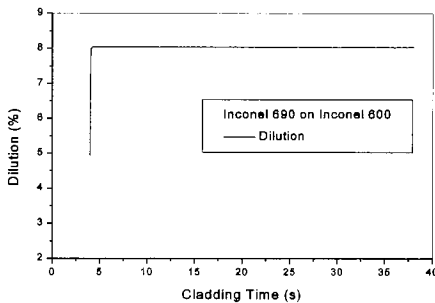


Fig. 8 The dilution of clad layer under the condition of controlling dilution

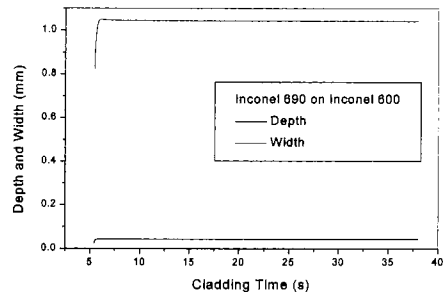


Fig. 9 The depth and width of melt pool under the condition of controlled dilution

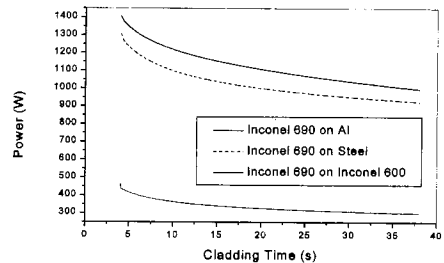


Fig. 10 The variation of power for controlled dilution

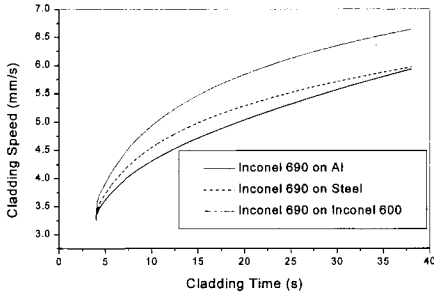


Fig. 11 The variation of cladding speed for controlled dilution

Al is higher than that needed for cladding of steel, and the laser power needed for cladding of steel is higher than that for cladding of Inconel 600. If the laser powers are kept constant, the cladding speeds have to be increased. Figure 11 shows the variations of cladding speeds for controlling the dilution when the laser powers don't change, as 1407W for cladding on Al, 1310 W for cladding on mild steel, and 456 W for cladding on Inconel 600. At first the cladding speeds increase rapidly and then the increase rates of cladding speeds become slower and slower.

5.3 Simulation of width control of melt pool

For in situ control of laser cladding, one or more reference parameters are needed as feedback parameters. The width of melt pool is one of the detectable parameters (Mohanty, P. S. and Mazumder, J., 1998). The question needs to answer is that whether the dilution can be controlled if the width of melt pool is controlled. The situation is simulated by the time-dependent finite element method with the adaptive mesh. Figure 12 shows the flowchart of the program for the width control of melt pool. At a given cladding time, the width of melt pool is computed. Then the input power is adapted by comparing the computed width with preset width limit. That is:

$P = P - \Delta P$, if the computed width is larger than the preset width limit.

$P = P + \Delta P$, if the computed width is smaller than the preset width limit.

This process repeats until the computed width

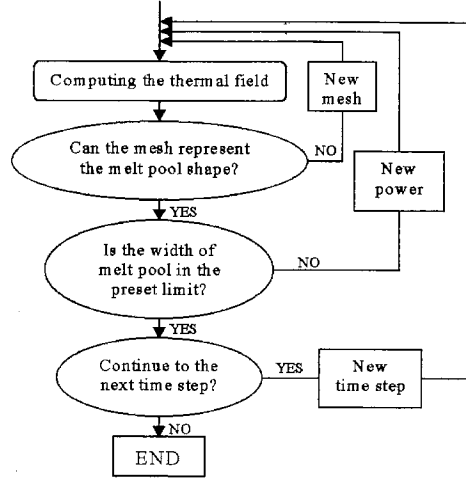


Fig. 12 Flowchart of program for width control of melt pool

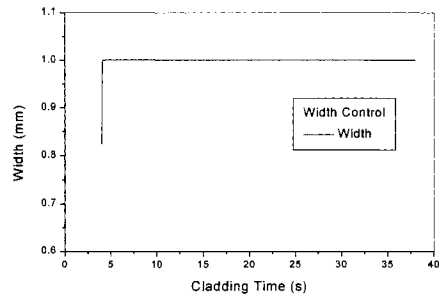


Fig. 13 The width of melt pool under the condition of controlling width

is in the preset width limit. Then the computation goes to the next time step and the above process repeats again. It should be pointed out that for some cladding materials, the width of clad layer may be larger than the width of melt pool in the base metal. The liquid metal may flow beyond the melting line of base metal and bond with the surface of base metal. In this model the width of melt pool refers to the width of melting line of base metal.

Figure 13 shows the controlled width when cladding Inconel 690 on Inconel 600. The width is controlled between 0.999 mm and 1.001 mm. The resulting dilution is shown in Fig. 14. At the very beginning, the dilution is a little unstable and then the dilution is kept stable. The unstable part of dilution at the very beginning is caused by the instability of depth of melt pool at the very

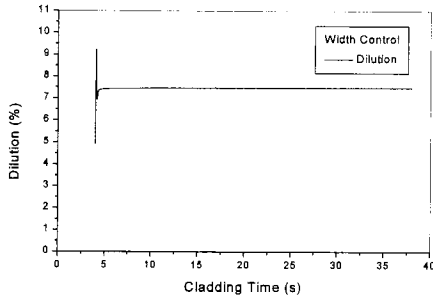


Fig. 14 The dilution of clad layer for controlled width of melt pool

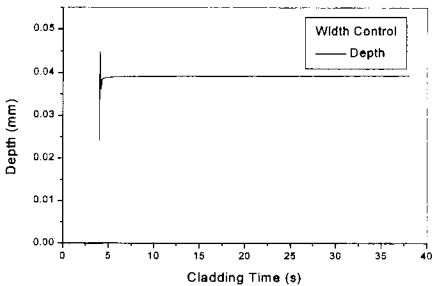


Fig. 15 The depth of melt pool for controlled width

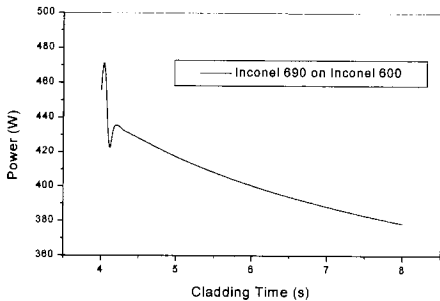


Fig. 16 The variation of power for controlled width

beginning, as shown in Fig. 15. The melt pool is required to form in 4 seconds. Before cladding the base metal is at room temperature. So a larger laser power is required at the beginning of cladding, as shown in Fig. 16, where the cladding speed is 3.33 mm/s. This power will cause rapid change of thermal field near the melt pool, resulting in deeper melt pool. The width will soon be larger than the preset width limit if the power is kept constant. The feedback command makes the power decrease rapidly. It results in a smaller depth of melt pool. After the formation of melt pool, the

thermal field changes in a stable rate, so the power decreases smoothly, and the depth and dilution of melt pool can be kept constant. The results indicate that the width of melt pool can be used as the reference parameter for dilution control.

6. Conclusions

(1) The changing melt pool and the modeled object can be well represented by adaptive mesh method during the time-dependent finite element method computation.

(2) If input line energy is kept constant, the dilution increases during laser cladding, especially at the beginning.

(3) Heat conductivity of base metal is an important parameter for laser cladding. Base metal with high heat conductivity needs high power for laser cladding.

(4) To keep dilution in a certain range, the input line energy should be reduced. The reducing rate of input line energy is fast at first few seconds and then becomes slower and slower. This can be realized by reducing laser power or increasing cladding speed.

(5) Dilution can be controlled if the width of melt pool is controlled.

References

- Agrawal, G., Kar, A. and Mazumder, J., 1993, "Theoretical Studies on Extended Solid Solubility and Nonequilibrium Phase Diagram for Nb-Al Alloy Formed During Laser Cladding," *Scripta Metallurgic et Materialia* 28, (11), 1453 ~ 1458.
- Atamert, S., and Bhadeshia, H. K. D. H., 1989, "Comparison of the Microstructures and Abrasive Wear Properties of Stellite Hardfacing Alloys Deposited by Arc Welding and Laser Cladding," *Metall. Trans. A* 20A, (6), 1037 ~ 1054.
- Chan, C., Mazumder, J. and Chen, M. M., 1984, "A Two-Dimensional Transient Model for Convection in Laser Melted Pool," *Metall. Trans. A*, Vol. 15A, pp. 2175 ~ 2184.
- Damborene, J. J., Vazquez, A. J., Lopez, V.,

- Weerasinghe, V. M. and West, D. R. F., 1993, "Laser Cladding of Austenitic Stainless Steel on Mild Steel—Microstructural and Corrosion Properties," *Processing of Advanced Materials* 3, (2), 107~113, ISSN: 0960-314X.
- David, S A; Vitek, J M; "Correlation Between Solidification Parameters and Weld Microstructures," *International Materials Reviews*, 1989, Vol. 34, No. 5, pp. 213~245.
- Denney, P. E. and Duhamel, R., 1998, "Update: Laser Beam Cladding with CO₂ and Nd:YAG Laser," *Industrial Laser Review*, No. 11, pp. 19~21.
- Fouquet, F., Sallamand, P., Millet, J. P., Frenk, A., Wagniere, J. D., 1994, "Austenitic Stainless Steel Layers Deposited by Laser Cladding on a Mild Steel, Realization and Characterization," *J. Phys. (France)* IV4, (C4), 89~92.
- Frenk, A., Henchoz, N., and Kurz, W., 1993, "Laser Cladding of a Cobalt-Based Alloy, Processing Parameters and Microstructure," *Zeitschrift Fur Metallkunde* 84, (12), 886~892. ISSN: 0044-3093.
- Hirose, A., Kohno, W., Nomura, D. and Kobayashi, K. F., 1992, "Formation of Hardfacing Clad by Laser Cladding with Blown Powder," *Tetsu-To-Hagane (Journal of the Iron and Steel Institute of Japan)* 78, (10), 1585~1592.
- Hoadley, A. F. A. and Rappaz, M., 1992, "A Thermal Model of Laser Cladding by Powder Injection," *Metall. Trans. B*, Vol. 23B, pp. 631~642.
- Kar, A. and Mazumder, J., 1988, "One-Dimensional Finite-Medium Diffusion Model for Extended Solid Solution in Laser Cladding of Hf on Nickel," *Acta Metall.* Vol. 36, No. 3, pp. 701~712.
- Kar, A. and Mazumder, J., 1989, "Extended Solution and Nonequilibrium Phase Diagram for Ni-Al Alloy Formed during Laser Cladding," *Metall. Trans. A*, Vol. 20A, pp. 363~371.
- Kim, J. D. and Subramanian, R. V., 1988, "Heat Flow in Laser Beam Welding," *4th Intl Conf. on Welding by Electron and Laser Beams*, Cannes France, pp. 175~182.
- Kim, J. D. et al., 1992, "The Behavior of Fracture Deviation in the Impact Test of Narrow Laser Welds," *Proc. of the Intl Symposium on Impact Engineering*, Sendai, Japan, pp. 455~460.
- Kim, J. D., Na, I. and Park, C. C., 1998, "CO₂ Laser Welding of Zinc-Coated Steel Sheets," *KSME International Journal*, Vol. 12, No. 4, pp. 606~614.
- Koshy, P., 1985, "Laser Cladding Techniques for Application to Wear and Corrosion Resistant Coatings," Conference: Applications of High Power Lasers, Los Angeles, California, USA, 22-23 Jan. 1985, Publ: SPIE, The International Society for Optical Engineering, P. O. Box 10, Bellingham, Washington 98227-0010, USA, 80~85.
- Li, L. J. and Mazumder, J., 1984, "Laser Processing of Materials (edited by K. Mukherjee and J. Mazumder)," pp. 35~50. *Proc. Metal. Soc. AIME*, Los Angeles, Calif.
- Liu, Y., Mazumder, J. and Shibata, K., 1994, "Laser Cladding of Nickel-Aluminum Bronze on Al Alloy AA333," *Metall. Mater. Trans. B* 25B, (5), 749~759.
- Mazumder, J. and Kar, A., 1987, "Solid Solubility in Laser Cladding," *J. Met.* 39, (2), 18~23.
- Mazumder, J., Sircar, S., Ribaudou, C. and Kar, A., 1992, "Laser Cladding of Non-Equilibrium Metallic Alloys," *Thermomechanical Aspects of Manufacturing and Materials Processing*, 319~335; Publ: Hemisphere Publishing Corp., 79 Madison Ave., New York 10016-7892, USA.
- Mohanty, P. S. and Mazumder, J., 1998, "Solidification Behavior and Microstructural Evolution during Laser Beam-Material Interaction," *Metall. Mater. Trans. B*, Vol. 29B, pp. 1269~1279.
- Ono, M., Kosuge, S., Nakada, K. and Watanabe, I., 1987, "Development of Laser Cladding Process," Conference: LAMP'87: Laser Advanced Materials Process-Science and Applications, Osaka, Japan, 21-23 May 1987; Publ: High Temperature Society of Japan, c/o Welding Research Institute of Osaka University, 11-1 Mihogaoka, Ibaraki, Osaka 567, Japan; 395~400.
- Ramous, E., Giordano, L., Tiziani, A., Badan,

B. and Cantello, M., 1989, "Laser Cladding of Ceramic and Metallic Coatings on Steel," *Conference: Surface Engineering With High Energy Beams: Science and Technology*, Lisbon, Portugal, 25-27 Sept. 1989; Publ: CEMUL, Av. Rovisco Pais, 1096 Lisboa Codex, Portugal, 425~433.

Tosto, S., Pierdominici, F. and Bianco, M., 1994, "Laser Cladding and Alloying of a Nickel-Base Superalloy on Plain Carbon Steel," *J. Mater. Sci.* 29, (2), 504~509.

Uenishi, K. and Kobayashi, K. F., 1993, "Laser

Cladding of Intermetallic Compound Al_3Ti on Aluminum Substrate," *Kei Kinzoku Yosetsu (Journal of Light Metal Welding and Construction)* 31, (4), 1~5.

Yang, X., Zheng, T., Zhang, N., Zhong, M., Lin, Y. and Gao, S., 1992, "Convection and Mass Transfer in Laser Cladding on FeCrSiB Alloy," *Acta Metallurgica Sinica (China)* 28, (2), B84~B88. ISSN: 0412-1961.

Yellup, J. M., 1995, "Laser Cladding Using the Powder Blowing Technique," *Surf. Coat. Technol.* 71, (2), 121~128, ISSN: 0257-8972.